Wear 304 (2013) 1–12

Contents lists available at SciVerse ScienceDirect

Wear

journal homepage: www.elsevier.com/locate/wear

Friction and wear performance of copper–graphite surface composites fabricated by friction stir processing (FSP)

H. Sarmadi *, A.H. Kokabi, S.M. Seyed Reihani

Department of Materials Science and Engineering, Sharif University of Technology, Azadi Street, Tehran, Iran

ARTICLE INFO

Article history:
Received 31 August 2012
Received in revised form
5 April 2013
Accepted 15 April 2013
Available online 30 April 2013

Keywords:
Sliding wear
Metal-matrix composite
Solid lubricants
Lubricant additives
Other surface engineering processes
Wear testing

ABSTRACT

Copper–graphite composites which have low friction coefficient can be used as bearing materials in lieu of materials containing lead which cause environmental problems. So far, some methods such as powder metallurgy and centrifugal casting have been employed to produce these composites. In this study, friction stir processing (FSP) was used to produce copper–graphite surface composites. Five tools with different pin profile were employed in order to achieve a comprehensive dispersion. Results show that the tool with triangular pin gives rise to a better dispersion of graphite particles. Furthermore, four copper–graphite composites containing different graphite content were prepared using triangular tool through repeating the process passes. Friction and wear performance of the composites were studied using a pin-on-disc tribometer. It was indicated that the friction coefficients of composites were lower than pure annealed copper and decreased with increase in graphite content. The reduction in friction coefficient is due to decrease in metal–metal contact points, originated from the presence of graphite particles as a solid lubricant. Wear loss of the composites was also decreased with increase in graphite content. This is related to change in wear mechanism from adhesive to delamination wear and reduction of friction coefficient.

© 2013 Elsevier B.V. Open access under CC BY-NC-ND license.

1. Introduction

Friction stir welding (FSW) is a solid-state joining technique which was devised at The Welding Institute (TWI) of UK in 1991 and at first was applied to aluminum alloys [1,2]. In FSW, a non-consumable rotating tool with a pin and a shoulder is inserted into the opening of joint in adjoining sheets or plates and traversed along the line of joint and cause plates to be joined [2]. Friction stir processing (FSP) has been recently developed by Mishra et al. [3,4] based on basic principles of FSW. In this case, a rotating tool is inserted in a monolithic work piece in order for modification of microstructure (Fig. 1). Furthermore, FSP technique has been employed by Mishra et al. [5] to produce surface composite on aluminum substrate. It is reported that process parameters such as tool geometry, rotating speed and transverse speed have a significant effect on production of surface composite layer [5]. FSP have also been employed to produce some other composites such as Al–Al_2O_3, AZ31–MWCNT (multi walled carbon nano tube), AZ61–SiO_2, Al–SiC, etc. [6–9].

In former times several different types of materials such as copper alloys like leaded bronzes, aluminum bronzes, phosphorus bronzes as well as aluminum alloys like aluminum–-tin and aluminum–silicon alloys have been reported to be studied for their tribological properties [10]. Most of the bearing alloys that were used so far had contained a soft phase like lead, which provide the required antifriction property. Because of its harmful effects on environment, restrictions have been imposed on lead use. This has made researchers find alternative materials, which have tribological properties similar to materials containing lead [10]. Self-lubricant composites such as aluminum–graphite, copper–graphite, and aluminum–MoS_2 composites have been reported to be investigated for tribological applications [10]. These metal matrix composites (MMCs) not only reduce friction coefficient but also reduce the wear of counterparts [10,11]. Graphite is very effective in reducing the wear and friction coefficient of the composites. By contrast, molybdenum disulfide (MoS_2) is ineffective as a solid lubricant for sintered composites due to its instability and reactivity with the metals at the sintering temperature [12].

Copper–graphite composites possess the properties of copper, i.e. excellent thermal and electrical conductivities, and properties of graphite, i.e. solid lubricating and low thermal expansion coefficient. These composites are widely used as brushes, and bearing materials in many applications [11]. Wear mechanism and friction coefficient of copper–graphite composites fabricated by powder metallurgy from Cu-coated and Cu-uncoated graphite particles containing 0–20 vol% of graphite was studied by Moustafa et al. [11]. They described that the involved wear mechanisms of pure

* Corresponding author. Tel.: +98 919 2710735; fax: +98 263 92108077.
E-mail address: hsn.sarmadi@yahoo.com (H. Sarmadi).

0043-1648 © 2013 Elsevier B.V. Open access under CC BY-NC-ND license.
http://dx.doi.org/10.1016/j.wear.2013.04.023

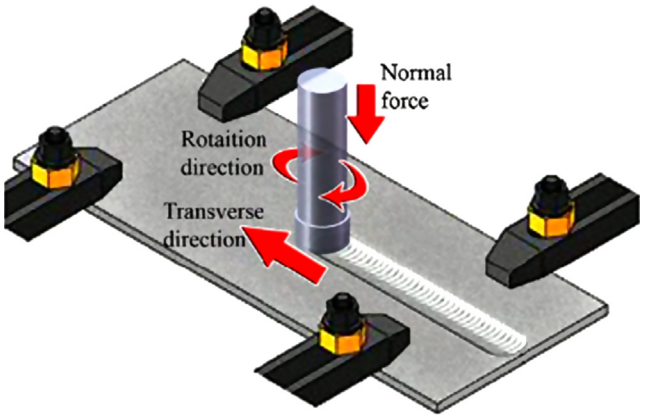

Fig. 1. Schematic illustration of FSP process [10].

copper at low, mild and severe wear regimes could be oxidative-dominated, delamination, and seizure wear mechanisms, respectively. However, both Cu-coated and uncoated graphite composites exhibited the same wear mechanisms, namely, oxidation induced delamination, high strained delamination and sub-surface delamination. They stated that at constant load the higher graphite content in either coated or uncoated Cu–graphite composite, the lower is the coefficient of friction. However, Rohatgi et al. [13] stated that when the graphite content of metal matrix composites is more than about 20 vol% the friction coefficient approaches that of pure graphite and becomes independent of the graphite content. Kovacik et al. [14] investigated the effect of composition on the friction coefficient of copper–graphite composites in the range of 0–50 vol% of graphite at constant load to determine critical graphite content above which the coefficient of friction of composite remains almost composition independent and constant. It was stated that with increase in concentration of graphite, the coefficient of friction and wear rate of coated and uncoated composites at first decreases and after reaching certain critical concentration threshold of graphite, the coefficient of friction of composites becomes independent of the composition and equal to the friction coefficient of used graphite material while the wear rate decreases further. This concentration threshold is determined to be 12 vol% and about 25 vol% in the case of composites with uncoated and coated graphite particles, respectively. Due to the complication of wear mechanisms, no general relationship between microstructural factors, processing parameters and the wear resistance of metal matrix composites could be established. Recent studies showed that in addition to the volume fraction of particles, spatial distribution of the graphite particles and particles size has a great effect on friction coefficient [14,15]. Furthermore, because of higher mechanical properties, in some studies carbon fibers and nanotubes have been employed in preference to graphite particles [16–20]. Apart from high strength and modulus, carbon fibers have good lubrication effect and wear resistance. The carbon fiber reinforces the matrix and improves the tribological properties of the composite as a solid lubricant. Therefore, the wear resistance of the carbon fiber-reinforced composites is much higher than pure metals [16]. In addition, the effect of graphite on high temperature wear has been investigated and it is reported that adding graphite particles to Cu–SiC composite prevent composites from high temperature severe wear [21].

So far, some methods such as powder metallurgy [11] and centrifugal casting [10,22] have been used to fabricate these composites. The most important problem of these methods is agglomeration of graphite particles. Because of lower density of graphite than copper, graphite particles tend to agglomerate into graphite clusters. In addition, being greasy is another reason for agglomeration of graphite particles. Coating graphite particles with copper by electro-less process leads to less agglomeration [11]. Residual porosity can also be present, since in both powder metallurgy and casting processes porosity may be present in the final product.

The aim of this research is using friction stir processing to produce Cu–graphite composite. Simultaneous stirring of materials during fabrication process which is one of the features of this process, can solve the agglomeration of graphite particles. Therefore, FSP was employed to produce these composites. Tribological properties of the composite were studied. The effect of graphite content on friction coefficient and wear loss of the composites as a main aim of the research were investigated.

2. Experimental procedure

2.1. Material and procedure

Commercial pure copper plates (100 mm × 60 mm × 5 mm in size) were used as substrates. The plates were annealed at 620 °C for 2 h. Graphite particles (average particles size 5 μm, purity 99.9%) were used as solid lubricant materials.

In order to prepare FSP tools, H13 tool steel was employed. The shoulder diameter was 20 mm and the pin was 3 mm in length and the pin diameter of all the tools was effectively 6.5 mm. Pin profile plays a vital role in material flow [23,24]. In this study (exactly the same as Elangovan and Balasubramanian [24]) five tools with different pin profiles (straight cylindrical (SC), tapered cylindrical (TC), threaded cylindrical (TH), square (SQ), and triangular (TR)) were applied which are shown schematically in Fig. 2. All of the tools were hardened in order to be prevented from wear. The hardness of tools after heat treatment was 52 ± 2 HRC.

A groove was machined on the surface of plates along the length of plate. The grooves were 0.9 mm in width. Then, graphite particles were added into grooves so that the grooves were completely filled. After that, plates were fixed on the FSP machine and at first, the surface of grooves were sealed by a tool without pin in order to prevent particles from coming out and being wasted. The FSP machine used here was a modified horizontal milling machine. And finally, specimens were FSPed by tools that had pin.

The main source of heat in FSP is friction between tool and work piece [2,25]. Since the objective of this study was fabrication of low friction coefficient copper base composites, there were two limitations: (1) high heat transfer coefficient of copper resulting in wasting produced heat (2) low friction coefficient of used material causing less heat production. To solve these problems, specimens were isolated and high rotating speed and low transverse speed were employed. Thus, rotating and transverse speed were 1600 rpm and 20 mm min^{-1} respectively and tool angle was 1.5 degree.

In order to increase in graphite content, specimens were subjected to repetitive passes of process, i.e. after grooving plates, filling with graphite particles, and FSPing them, the specimens were grooved, filled with graphite particles and FSPed again. Using this procedure, copper–graphite composites with 1, 2, 3, and 4 passes were produced. For specimens prepared by different tools, two passes were applied. The reason of using two passes of process was making more difference in order to compare better. Furthermore, a pure copper plate without graphite particles was prepared as a representative sample and its friction coefficient and wear loss were measured and compared with copper–graphite composites. Table 1 shows all the specimens produced in this study.

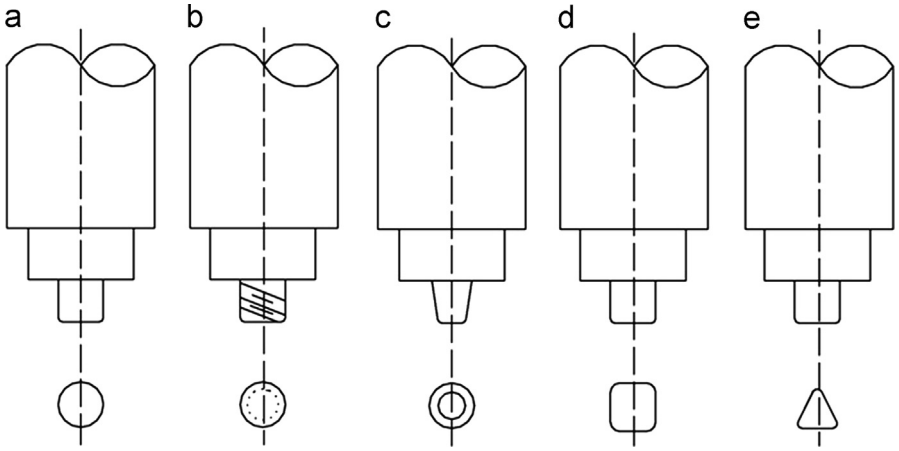

Fig. 2. FSP tool pin profile [24]. (a) Straight cylinder(SC), (b) Threaded cylindrical(TH), (c) Tapered Cylindrical(TC), (d) Square(SQ) and (e) Triangle(TR).

Table 1
Produced specimens.

No.	process	Specimens
1	FSPed by Straight Cylindrical pin	Cu-2G-SC
2	FSPed by Tapered Cylindrical pin	Cu-2G-TC
3	FSPed by Threaded Cylindrical pin	Cu-2G-TH
4	FSPed by Square pin	Cu-2G-SQ
5	FSPed by Triangular pin	Cu-2G-TR
6	FSPed by Triangular pin(one pass)	Cu-1G
7	FSPed by Triangular pin(two passes)	Cu-2G=Cu-2G-TR
8	FSPed by Triangular pin(three passes)	Cu-3G
9	FSPed by Triangular pin(four passes)	Cu-4G
10	Pure copper annealed at 620 °C for 2h	Pure Annealed Copper

2.2. Friction coefficient and wear test

Friction coefficients and wear properties of specimens were measured using pin-on-disk tribometer. A steel disk (SAE1045) according to ASTM G99 standard was prepared and heat treated to be hardened. The hardness of disk after heat treatment was 60 ± 2 HRC ($\sim$700 HV). After that, the surface of disk was polished and the roughness of surface was measured, $R_{max} = 0.6$ μm. Cylindrical specimens were wire cut along composites thickness with 5 mm in diameter from center of composites. For specimens prepared by different tools (specimen 1 to 5) one pin was also cut from 3 mm beside centerline of specimens. The pins were then polished and cleaned by acetone to remove all the contamination before testing. All the tests were carried out at the temperature of 20 ± 2 ℃ and ambient humidity ($\sim$50%). The nominal load and sliding speed were 10 N and 0.3 ms^{-1}, respectively. In friction coefficient test the sliding distance for all the specimens was 1000 m and friction coefficient was determined by tribometer automatically. In wear test specimens were initially weighed on the digital scales with 0.0001 g accuracy and then were tested for 100 m and weighed again. This procedure was performed for 1000 m (10 steps-three times for each individual testing condition) and wear loss and wear rate of specimens were determined as average of three measurements. Wear rate of specimens was measured using following equation

$$W = \frac{M}{LD} \quad (1)$$

where W is wear rate (g/N m), M is the wear loss (g), L is the applied load (N), and D is sliding distance (m).

2.3. Microscopic and hardness examinations

Metallographic investigation was carried out using both optical and scanning electron microscopes. SEM (scanning electron microscopy) and EDS (energy dispersive spectroscopy) analysis was used for both pin and disk to determine wear mechanism. Vikers microhardness of specimens was also measured using 50 g load for 10 s applying on cross-section of each specimen.

3. Results and discussion

3.1. Effect of tool geometry on particle dispersion and friction coefficient

Fig. 3 shows optical micrographs of particles distribution on the surface of samples 1 to 5. These images have been taken from center of composites' surface. As can be seen, in the case of composites produced by tools with straight cylindrical, tapered cylindrical, and threaded cylindrical pins, i.e. Cu-2G-SC, Cu-2G-TC, and Cu-2G-TH, respectively, particles have aggregated in the center of composites, but in the case of composites produced by tools with square and triangular pins, i.e. Cu-2G-SQ and Cu-2G-TR, respectively, particles have totally dispersed in the matrix and the distribution of particles is adequate.

This is related to flow patterns of copper substrate against different tools during FSP. Three microscopic images were taken from center of each composite and then particles volume percents and particles size after process were determined by Image Analyzer software represented in Table 2. These results confirm microscopic observations. According to Table 2, particles volume percent has a maximum value in composite produced by SC pin being 13.95%, but in the case of composite produced by TR pin, this is 10.89 vol% which is minimum value among all of the composites. Composite produced by SQ pin has 11.90 vol% graphite particles which is lower than composites produced by SC, TC, and TH pins. Lower particles volume percent of composites produced by SQ and TR pins shows that particles have not aggregate in the center of these composites and distribution of particles on surface of these composites is better than three other composites. The size of largest cluster in Cu-2G-SC, Cu-2G-TC, and Cu-2G-TH composites is more than 40 μm which proves that particles have agglomerated and as can be seen from Fig. 3a–c, the amount of these clusters are high. In the case of Cu-2G-SQ and Cu-2G-TR composites, the size of largest cluster is about 27 and 22 μm, respectively which are

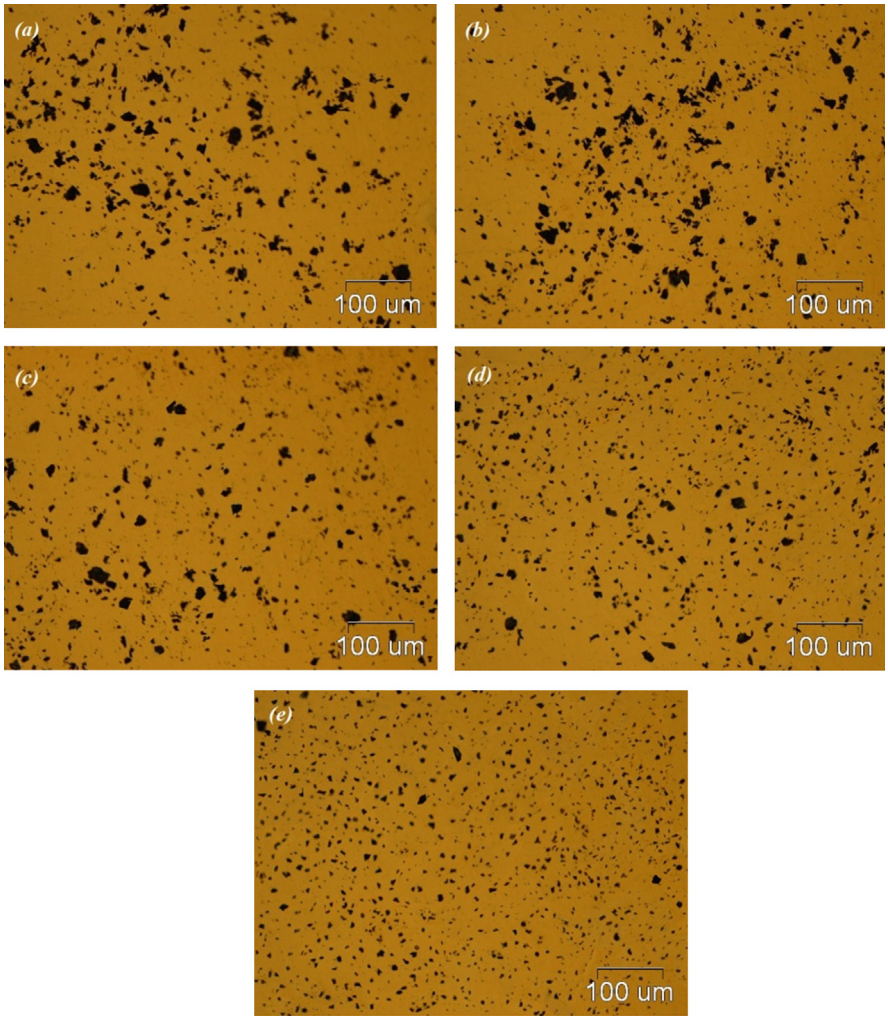

Fig. 3. Optical microscopic images from center of (a) Cu-2G-SC, (b) Cu-2G-TC, (c) Cu-2G-TH, (d) Cu-2G-SQ, (e) Cu-2G-TR composites.

Table 2
Image Analyzer results obtained from center of composites.

Applied tool	SC	TC	TH	SQ	TR
Graphite particles content (vol.%)	13.95	13.80	12.32	11.90	10.89
Minimum particle size (μm)	1.50	1.50	1.50	1.50	1.50
Maximum particle size (μm)	44.20	52.00	43.30	27.30	21.90
Mean particles size (μm)	6.60	5.70	5.54	5.51	5.07

almost the same, but as can be seen in Fig. 3d and e, in Cu-2G-SQ composite, the amount of these clusters are more than those of TR pin.

Since the volume of grooves was constant, graphite content added into grooves was also constant and therefore, increase in particles volume percent in center of Cu-2G-SC, Cu-2G-TC, and Cu-2G-TH composites indicates that this parameter is decreased in adjacent areas of center of composite. Fig. 4 shows optical microscopic images of particle distribution in adjacent areas of composites surfaces. These images were taken from 3 mm beside centerline of composites. These images show that graphite particle content are higher in the case of Cu-2G-SQ and Cu-2G-TR composites indicating that particles are better dispersed and the composite area is larger.

Three images were taken from adjacent areas of composites' center and particles volume percents and particles size after process were determined by Image Analyzer software which results are represented in Table 3. Results show that graphite content for Cu-2G-SQ and Cu-2G-TR composites is higher than three other composites. Comparing Tables 2 and 3 show that difference between graphite contents in center and adjacent areas of center of Cu-2G-SQ and Cu-2G-TR composites is lower than that three other ones. In the case of composite produced by TR pin, this difference does not exceed even 1 vol%. This difference is 3 and 4 vol% for composites produced by SQ and TH pins respectively. This difference will deteriorate into 6 vol% using SC and TC pins. It is also proved that the size of the largest cluster and average of particles size is lower in Cu-2G-TR composite indicating more homogeneity of this composite. Consequently, better distribution of particle is reached using tool with triangular pin.

Friction coefficients of these five composites were determined from their center and adjacent areas of center using pin-on-disk tribometer to confirm microscopic observation in tool selection. For instance, Fig. 5 shows result of friction coefficient test for center of Cu-2G-TR composite. All of friction coefficient diagrams contain two stages like Fig. 5 named: (1) run-in (2) steady state stage. In run-in stage, friction coefficient increases continuously and in steady state stage, friction coefficient constantly oscillates within a certain range. Formation of run-in stage can be related to increase of the contact area, work hardening effect of wear and accumulating of debris in interface of pin and disk and change of wear mechanism from two-body to three-body wear [26]. Friction coefficient data were recorded by tribometer system in each 0.03 m. Reported friction coefficient in this study is average of these data in steady state stage. Table 4 represents average friction coefficient of all composites.

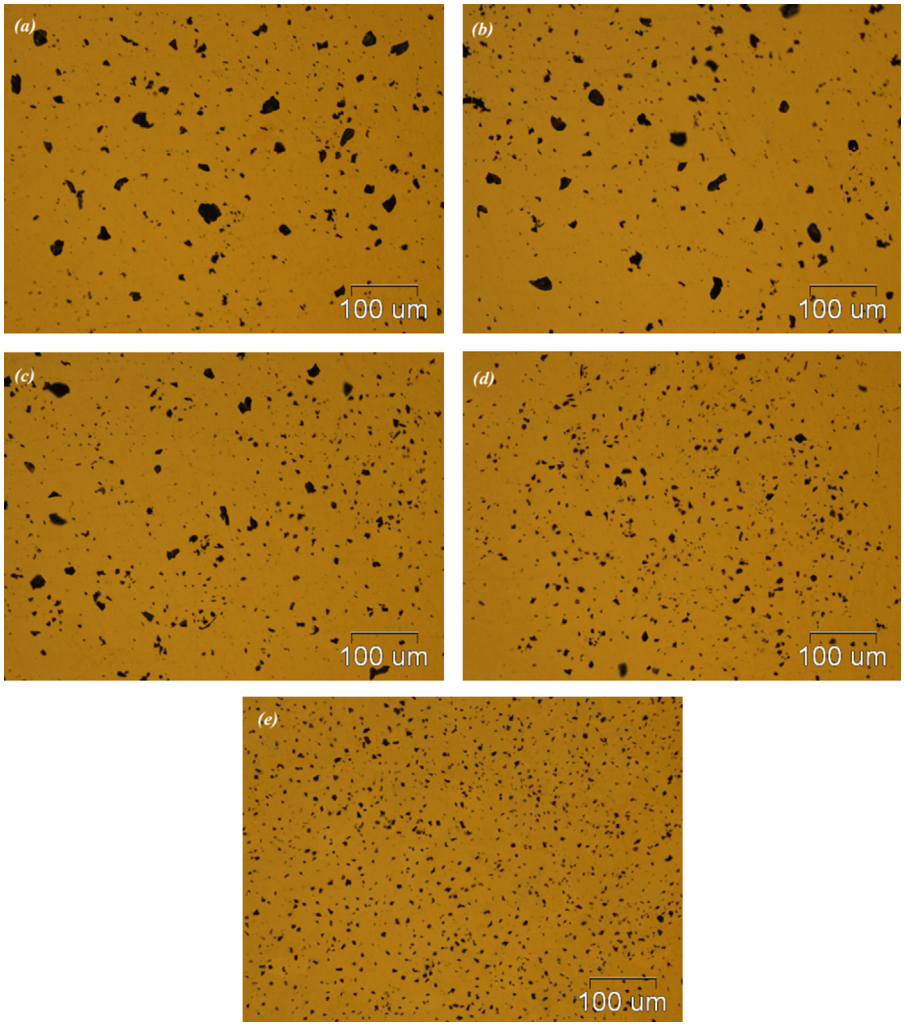

Fig. 4. Optical microscopic images from adjacent areas of center of (a) Cu-2G-SC, (b) Cu-2G-TC, (c) Cu-2G-TH, (d) Cu-2G-SQ, (e) Cu-2G-TR composites.

Table 3
Image Analyzer results obtained from adjacent areas of center of composites.

Applied tool	SC	TC	TH	SQ	TR
Graphite particles content (vol.%)	7.08	7.28	8.67	9.06	10.18
Minimum particle size (μm)	1.50	1.50	1.50	1.50	1.50
Maximum particle size (μm)	39.80	36.10	38.20	24.00	20.5
Mean particles size (μm)	5.35	5.36	5.22	5.13	5.07

As can be seen from Table 4, friction coefficient of composite produced by tool with triangular pin has the highest value (0.3) in center of composite due to lower graphite content and the lowest value (0.35) in adjacent areas of center of composite due to higher graphite content rather than other specimens. In other words, difference between friction coefficient of center and adjacent areas of center of this composite is lower than other composites indicating better distribution of particles in this specimen. Therefore, friction coefficient data confirm microscopic observations.

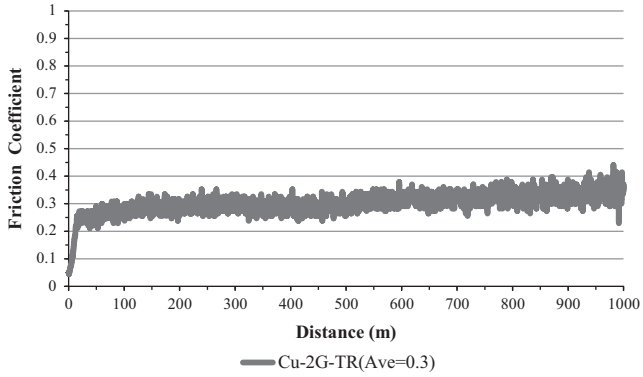

Fig. 5. friction coefficient of Cu-2G-TR composite obtained from center of specimen.

3.2. *Effect of graphite content on tribological performance of copper–graphite composites*

3.2.1. *Friction coefficient behavior*

Optical microscope images of Cu-1G, Cu-2G, Cu-3G, and Cu-4G composites are shown in Fig. 6.

Table 4
Friction coefficient of composites.

Composite type	Friction coefficient of center	Friction coefficient of adjacent areas of center
Cu-2G-SC	0.28	0.39
Cu-2G-TC	0.28	0.39
Cu-2G-TH	0.29	0.37
Cu-2G-SQ	0.29	0.37
Cu-2G-TR	0.30	0.35

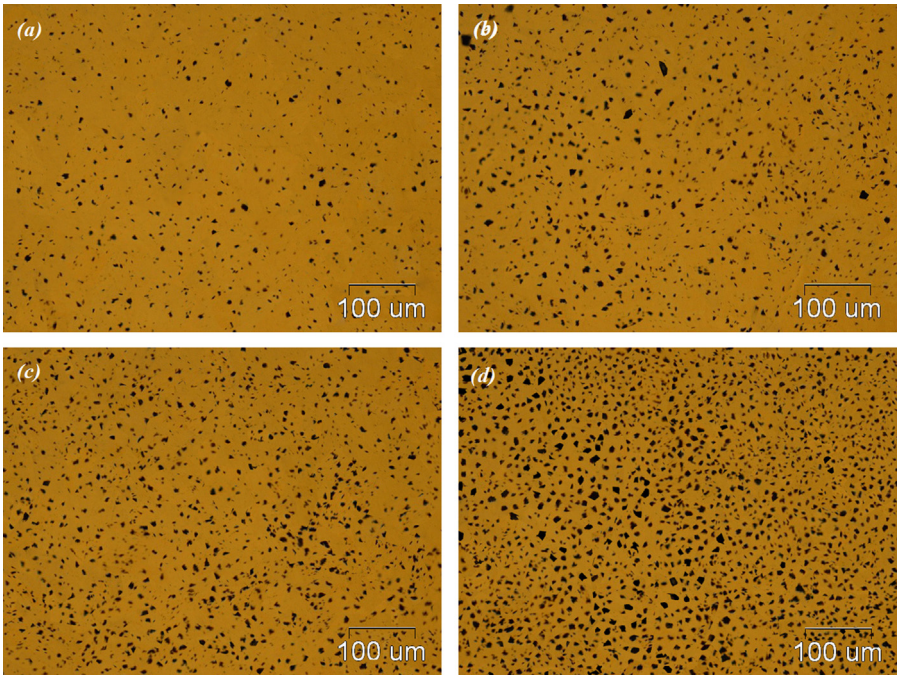

Fig. 6. Optical microscopic images from center of (a) Cu-1G, (b) Cu-2G, (c) Cu-3G, (d) Cu-4G composites.

Table 5
Image Analyzer results obtained from center Cu-1G, Cu-2G, Cu-3G, and Cu-4G composites.

Applied tool	Cu-1G	Cu-2G	Cu-3G	Cu-4G
Graphite particles content (vol.%)	6.54	10.89	16.70	22.12
Particle minimum size (μm)	1.5	1.5	1.5	1.5
Particle maximum size (μm)	20.3	21.9	22.9	31.6
Particles mean size (μm)	4.35	5.07	5.39	6.99

Three images were prepared from center of each individual composite and then particles volume percents and particles size after process were determined by Image Analyzer software represented in Table 5. As it was anticipated, with increase in number of process passes the volume percent of particles was increased from 6 vol% for one-pass to about 22 vol% for four-pass specimens. It is also clear that particle average size and the size of largest cluster are increased as the graphite volume percent increases showing that the particles tend to change into clusters as the graphite volume percent increases.

Microhardness data are represented in Fig. 7. According to these data, the average hardness of Cu-1G, Cu-2G, Cu-3G, and Cu-4G composites are 133, 128, 118, and 101 HV, respectively. In other words, the hardness of composites is reduced when graphite content increases which is due to presence of softer graphite particle in comparison with the copper matrix [12].

The results of friction coefficient test for the composites and pure annealed copper are shown in Figs. 8 and 9, respectively. As can be seen, the average of friction coefficient is decreased with increase in number of process passes or graphite content.

The friction coefficient values and the percent of its reduction for each pass are indicated in Table 6. It is clear that friction coefficient is dramatically decreased with increase in graphite content so that friction coefficient of Cu-4G composite containing about 22 vol% graphite is 79% lower than pure annealed copper. This is due to presence of graphite as a solid lubricant.

Due to mutual sliding of wear counterparts, graphite particles are smeared over contact surface and regarding good lubricating property of graphite, friction coefficient is decreased. In fact, graphite decreases metal to metal (composite to steel disk) direct

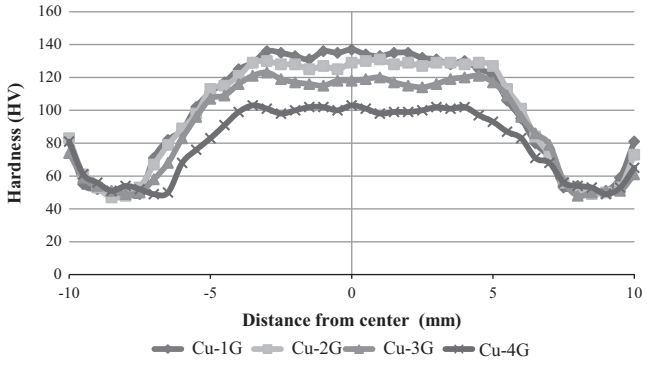

Fig. 7. Microhardness of Cu-1G, Cu-2G, Cu-3G, and Cu-4G composites.

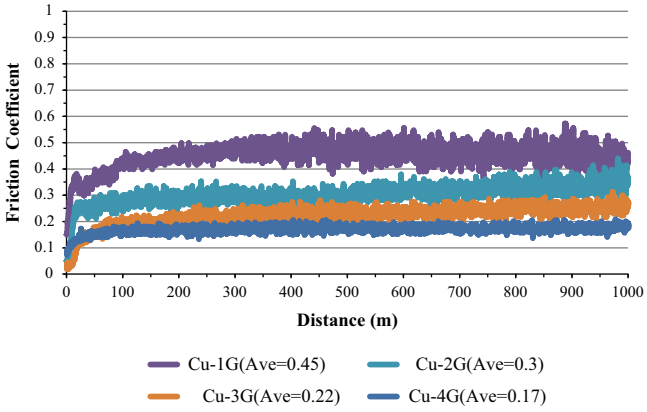

Fig. 8. Friction coefficient behavior of Cu-1G, Cu-2G, Cu-3G, and Cu-4G composites.

contact points leading to decrease in friction coefficient [12,18,19] and graphite has hexagonal structure and its atomic bonds in basal planes are covalent which are very strong, but atomic bonds between basal planes are van der Waals which are weak. These weak bonds are easily broken by low load. In other words, shear strength of graphite is too low leading to sliding of the planes over

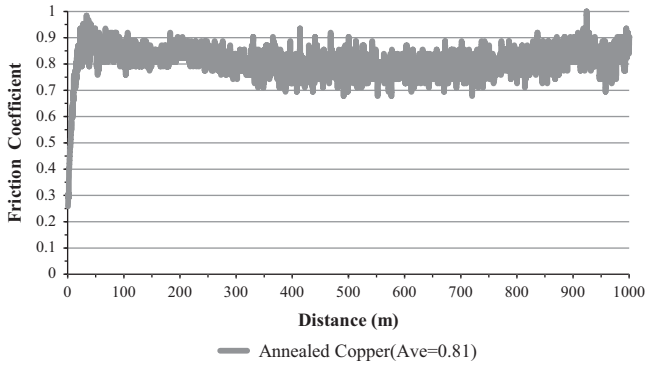

Fig. 9. Friction coefficient behavior of pure annealed copper.

Table 6
Friction coefficient variations of the specimens.

Specimen type	Friction coefficient	Reduction of friction coefficient in each pass (%)	Total reduction of friction coefficient against pure copper (%)
Pure annealed copper	0.81	-	-
Cu-1G	0.45	44.4	44.4
Cu-2G	0.30	33.3	62.9
Cu-3G	0.22	26.7	72.8
Cu-4G	0.17	22.7	79.0

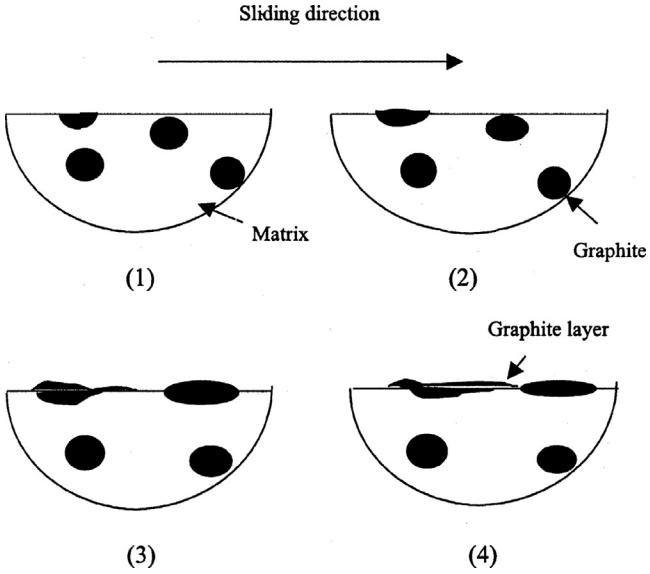

Fig. 10. Schematic illustration of the graphite particles squeezed out and smeared to the surface of composite [22].

each other and decrease in friction coefficient. Another feature of graphite that leads to reduction in friction coefficient is sticking of graphite particles to sliding surfaces; therefore, sliding take place within interior layers of graphite particles, so sliding of counterparts over each other is facilitated. Another point is that because of low hardness of graphite rather than copper and steel, wear does not occur in counterparts; therefore, friction coefficient is not increased. In addition to graphite present in surface of composite, graphite particles present in subsurface layer are also squeezed out to surface during sliding and increase covered areas of surface by graphite [22]. One of the important points in use of graphite as a solid lubricant is applying graphite particles continuously during sliding. Fig. 10 schematically shows squeezing out of graphite particles to surface of composite. According to Fig. 10, if matrix possesses low strength and high plastic deformation capability, squeezing out of graphite particles to surface will be eased. Since in this study the matrix is copper and has a good plastic deformation capability, squeezing out of graphite particles to surface is very likely taken place. In addition, amount of graphite squeezed out to surface is probably related to the mechanical properties of matrix, the morphology of graphite, the temperature in sliding surface, and more importantly, the bond between graphite particles and matrix. Due to low solubility of carbon in copper (it does not exceed 0.02 at%), there is no chemical and metallurgical bonding between copper and graphite atoms and the bond between them is only very weak mechanical bonding, therefore, separating of graphite particles from copper matrix and movement of them to sliding surface do not need considerable force [14]. However, because of the fact that graphite is softer than copper matrix, the bonding between graphite and matrix has less effect on amount of graphite squeezed out to surface rather than plastic deformation capability of matrix [22]. It is clear that the smaller the size of particles and the better their distribution are, the easier they are squeezed out.

As mentioned above, graphite particles are squeezed out to surface from matrix during sliding and this graphite and the graphite existed on the surface are smeared over counterparts interface as a layer. With increase in graphite content in composite, this layer becomes thicker and denser leading to decrease in friction coefficient and wear rate [11]. In fact, a tribolayer is formed on sliding interface which covers the surface. This layer is called mechanical mixed layer (MML). MML reduces the direct contact surface between composite and disk and so friction coefficient and wear loss are decreased. Copper, graphite, oxygen, and atmosphere moisture are the components of MML in copper–graphite composites. Since graphite is good lubricant, presence of small amount of it causes friction coefficient to be dramatically decreased (Table 6). In low graphite content, the particles form apart clusters (flakes) in MML. With increase in graphite content, MML become graphite-rich layer and graphite is not apart clusters anymore. This decreases friction coefficient even more.

Although, friction coefficient decreases to some extent as graphite content increases and after a threshold value of graphite content, it remains constant. There are some different values reported as the threshold. For instance, Rohatgi et al. [13] stated that when graphite content exceeds 20 vol%, friction coefficient approaches pure graphite friction coefficient and becomes independent of composite chemical composition. However, Kovacik et al. [14] studied the effect of graphite content on friction coefficient on copper–graphite composites. It is reported that there are some key parameters influencing on composition-dependent friction coefficient such as particles size and spatial distribution of graphite particles. It is clear that in low graphite contents, the smaller particles and the more homogenous are, the lower friction coefficient is. Thus, friction coefficient is decreased to a threshold and then remains constant even if graphite volume percent decreases. The most likely reason is that in threshold graphite content, other debris forming MML such as Cu_2O and copper particles have no effect on tribological behavior of MML and these properties are controlled by graphite particles. This graphite-saturated MML prevent subsurface area from significant deformation and therefore, shear strength of area close to surface and consequently friction coefficient remains nearly constant.

According to Table 6 and as can be seen from Fig. 11, reduction of friction in each step (pass) decreases demonstrating that friction coefficient is approaching a constant value as graphite content increases. Some suitable equations can be fitted with diagram of Fig. 11.

Here, both exponential and third-degree polynomial equations (as below) were derived according to the diagram indicating in Fig. 12, respectively. These equations govern over frictional behavior of copper–graphite composite according to graphite volume

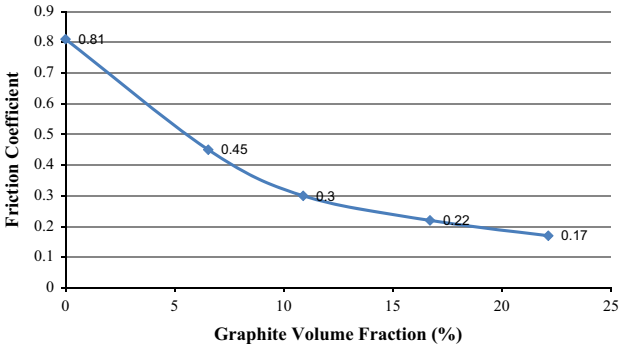

Fig. 11. Friction coefficient variations according to graphite content.

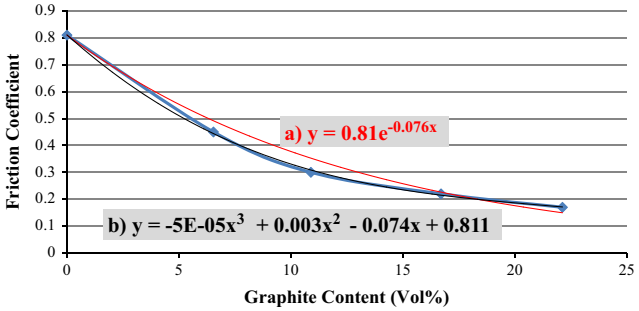

Fig. 12. Fitting equations representing frictional behavior of copper–graphite composite (a) exponential equation and (b) third-degree polynomial equation.

percent

$$y = 0.81e^{-0.076x} \quad (2)$$

$$y = -5E{-}05x^3 + 0.0031x^2 - 0.0743x + 0.81 \quad (3)$$

where y is friction coefficient and x is graphite volume percent. It shall be noted that these equations have been derived considering no microstructural effect on friction coefficient.

As mentioned before, in threshold graphite content, friction coefficient approaches a constant value approximately equal to friction coefficient of pure graphite. Friction coefficient of pure graphite is in range of 0.1–0.15 depending on load and test conditions (environment conditions). Since in this study, the load is 10 N which is nearly small, it can be assumed that friction coefficient of pure graphite possesses the lowest value being 0.1. If in exponential equation $y=0.1$, the threshold graphite content would be 27.52 vol%. Although this equation has a tangent in $y=0$, but as we know, friction coefficient is not allowed to be lower than 0.1, typical value for pure graphite. Therefore, this exponential equation can be used just for predicting the friction coefficient in concentration lower than threshold graphite content and is not applied to calculating the threshold. In a same way, if in third-degree polynomial equation $y=0.1$, the threshold graphite content would be 25.65 vol% which lower than that exponential equation. Thus, the threshold for graphite content in this study is about 25 vol%.

3.2.2. Wear behavior

Wear test was carried out on the specimens according to the procedure mentioned in Section 2.2. Fig. 13 shows variations of wear loss against sliding distance. These curves consist of two stages known as (1) running-in wear and (2) steady-state wear. Running-in wear ends when an equilibrium contact surface is established between the counterparts and a work hardened area is formed near the surface. In this stage, an adhesive oxide layer can

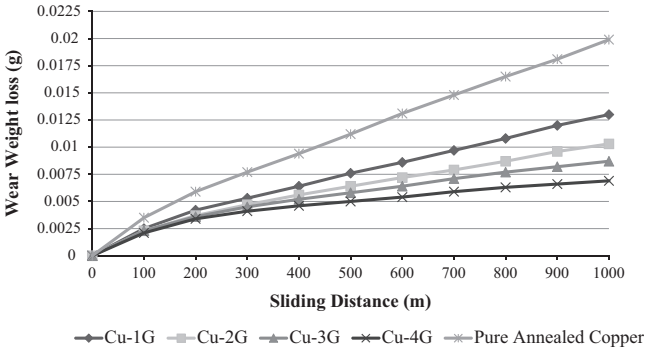

Fig. 13. Wear behavior of the specimens.

Table 7
Wear loss variations of the specimens.

Specimen type	Wear loss (in 1000 m) (g)	Reduction of wear loss in each pass (%)	Total reduction of wear loss against pure copper (%)
Pure annealed copper	0.0199	-	-
Cu-1G	0.0130	35	35
Cu-2G	0.0103	21	48
Cu-3G	0.0087	16	56
Cu-4G	0.0069	21	65

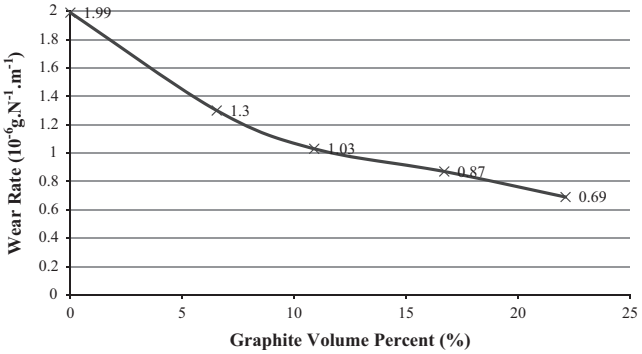

Fig. 14. Wear rate variations against graphite content.

prevent specimens from severe wear. In next stage, wear rate (curves slope) remains constant due to formation of a stable contact surface between counterparts. As can be seen, the wear loss of specimens is decreased with increase in graphite content.

Wear loss values after 1000 m sliding and the percent of its reduction for each pass are indicated in Table 7. Wear loss of pure copper after 1000 m sliding is about 0.0199 g, but this has changed to 0.0069 for Cu-4G composite i.e. adding about 22 vol% graphite to copper increases wear resistance of the composite by 65%. This is due to presence of graphite as a solid lubricant. As mentioned before, friction coefficient of the Cu-4G composite is decreased by 79% in comparison with pure copper. On the other hand, in some materials, reduction of friction coefficient leads to increase in wear resistance. Comparison between 65 and 79% reduction in wear loss and friction coefficient, respectively, shows that there is not a linear correlation between increase in wear resistance and decrease in friction coefficient. This needs more investigation of wear mechanism.

Average wear rate of specimens after 1000 m is plotted against graphite content in Fig. 14. It is clear that wear rate is decreased as graphite content is increased.

SEM image of worn surface of pure copper and EDS analyses of worn surface of the specimen and counterpart running against

specimen (wear disk) are shown in Figs. 15–17, respectively. As can be seen from Fig. 15, there is a high amount of plastic deformation in worn surface being one of the prominent characteristics of adhesive wear. During wear test, copper pin and steel disk have contact with each other in some projections. These contact points are deformed during wear process and form a solid state joint. This makes sliding more difficult for counterparts leading to increase in friction coefficient and wear loss. Adjacent area of contact points (adhesive area) is harden due to repetitive deformation resulting in formation of micro cracks in imperfections such as cavities and dislocations. These micro cracks then grow and lead to detachment of surface layer and as a result, intensive adhesive occurs [16,17,19,20] and these cracks can easily be seen in deformed area of Fig. 15. Therefore, the reason of high wear loss of pure annealed copper is occurrence of adhesive wear.

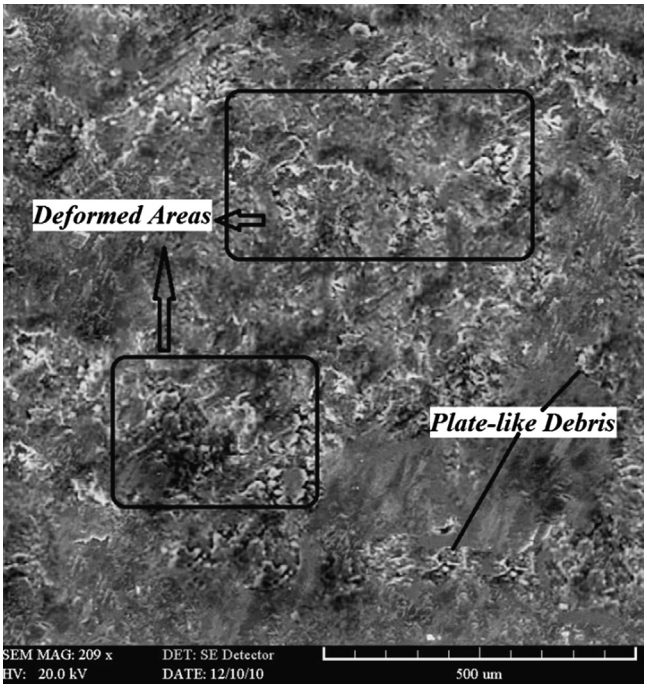

Fig. 15. SEM image of worn surface of pure copper pin.

In addition to large amount of deformation in wear surface, mass transfer between pin and disk is another characteristic of adhesive wear [20]. Friction force originates in metal joining in contact points. It is demonstrated that the strength of these joining can be as strong as counterparts and so rupture can happen in the distance below the junction inside of the counterparts. This causes material to be transferred from one part to another. Commonly, mass transfer happens mutually between pin and disk. Although, in the case of counterparts which there are a high difference in their hardness, mass transfer is from softer part to harder one [20]. The hardness of pure annealed copper is much lower than steel disk and so mass transfer is from copper pin to steel disk. EDS analysis of worn surface of copper pin show presence of no iron element and on the other hand, EDS analysis of wear disk running against copper pin show a high amount of copper element representing high mass transfer from pin to disk. This high mass transfer proves occurrence of adhesive wear.

Also, presence of plate-like debris in Fig. 15 is undeniable which one of characteristics of delamination wear. The amount of these debris is lower than deformed area. Presence of oxygen in EDS analyses of counterparts shows that a small amount of oxidation wear most likely has occurred. As can be seen, the dominant wear mechanism of pure annealed copper is adhesive and a small amount of delamination and oxidation happen beside.

SEM image of worn surface of Cu-1G specimen and EDS analyses of worn surface of the specimen and counterpart running against specimen (wear disk) are shown in Figs. 18–20, respectively. As can be seen from Fig. 18, a small amount plastic deformation has happened on wear surface and the majority of wear surface is formed of large plate-like debris indicating that

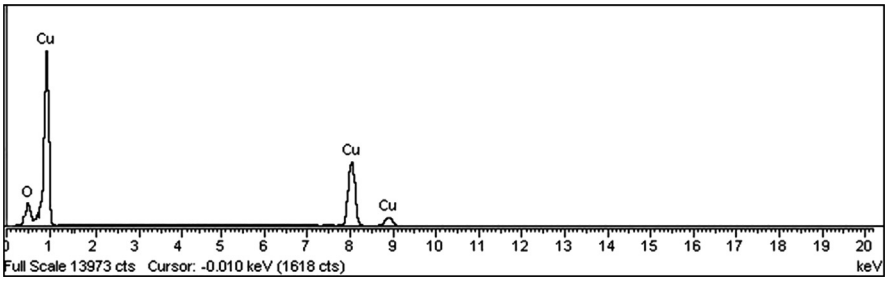

Fig. 16. EDS analysis of pure copper worn surface.

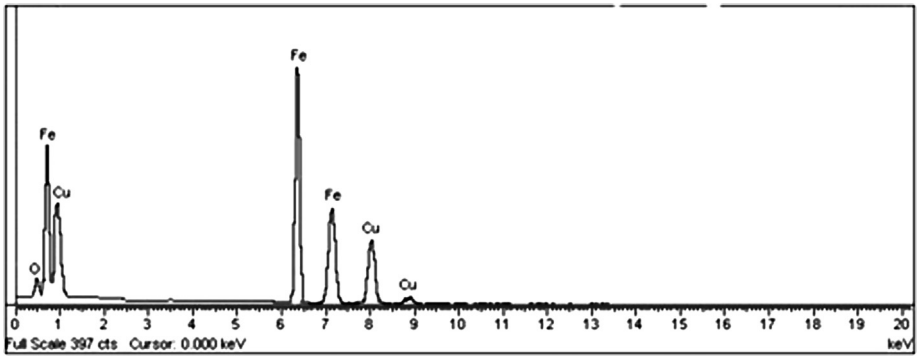

Fig. 17. EDS analysis of counterpart (wear disk) running against pure copper pin.

probably the wear mechanism is mainly delamination and adhesive wear has taken place less than pure copper.

EDS analysis counterpart running against Cu-1G pin (Fig. 20) shows small copper and carbon peak showing that mass transfer from pin to disk and as a result adhesive wear has occurred less in comparison with pure copper. Although, presence of oxygen in EDS analysis of Figs. 19 and 20 show that oxidation wear has probably occurred. The reason for reduction in adhesive wear is presence of graphite particle and decrease in number of metal to metal contact points.

Fig. 18. SEM image of Cu-1G worn surface.

Formation of plate-like debris and occurrence of delamination wear can be explained with respect to delamination wear theory. In delamination wear, the substance is considered as layered (laminated) which is detached from surface due to wear process. According to delamination wear theory, shear plastic deformation causes nucleation and growth of crack to be happened in a bit depth of the surface and these cracks eventually join together leading to detachment of layered area. In fact, accumulation of dislocations beneath the surface results in formation of pores in subsurface area (although because of severe plastic deformation resulted from FSP process, dislocations density in subsurface area is initially and before wear process high). These pores can also be formed in interface between graphite particles and copper due to absence of chemical bonds between graphite and copper. Joining of these pores leads to formation of cracks and subsequent growth during wear process results in formation of plate-like debris.

On the other side, in addition to above mechanism, another reason can be stated to explain delamination wear of copper–graphite composites. As mentioned before, graphite particles are squeezed out to composite surface during wear process. Thus, aggregation and accumulation of graphite on surface and subsurface area result in reduction of shear strength of subsurface area and because of sliding during wear process; these regions are detached from the surface as thin layers. Laminating of MML can also lead to delamination wear on the wear surface.

SEM image of worn surface of Cu-4G specimen and EDS analyses of worn surface of the specimen and counterpart running against specimen (wear disk) are shown in Figs. 21–23, respectively. As can be seen from Fig. 21, with increase in graphite content from 6 to 22 vol%, small plastic deformed area observed in

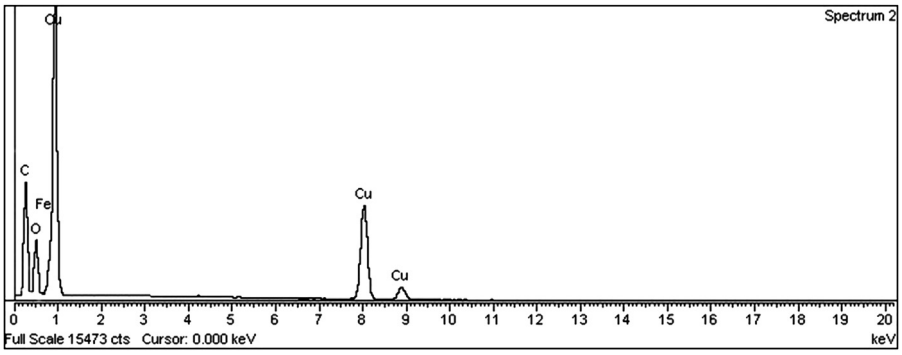

Fig. 19. EDS analysis of Cu-1G worn surface.

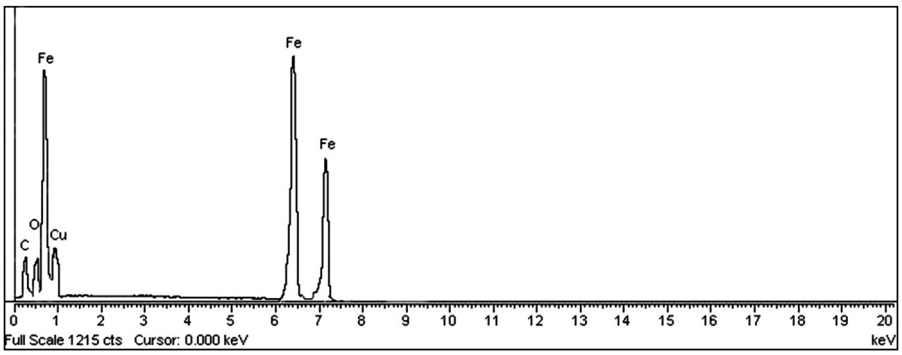

Fig. 20. EDS analysis of counterpart (wear disk) running against Cu-1G pin.

Fig. 18 is disappeared and delamination wear characteristics is observed almost in whole area.

In addition, the size of these plate-like debris is decreased with increase in graphite content. Although, EDS analysis of counterpart running against the specimen (Fig. 23) shows a short copper peak (small amount of copper) indicating occurrence of a small amount of adhesive wear.

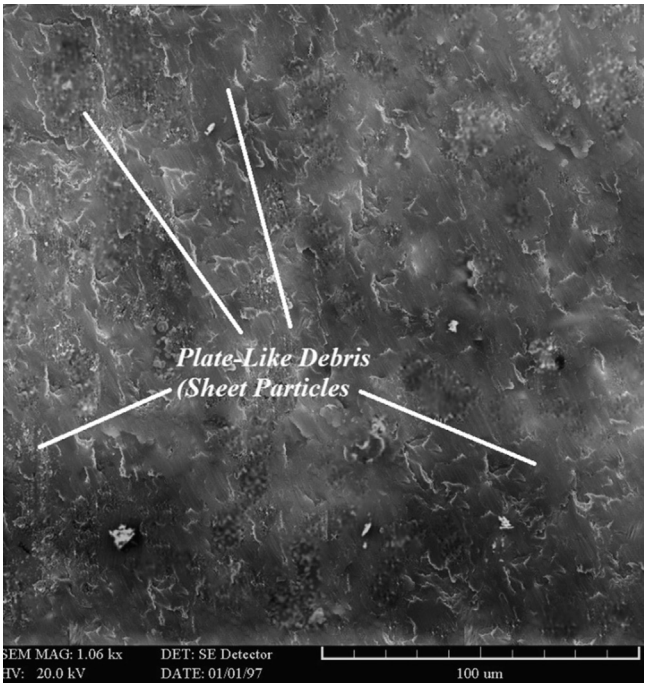

Fig. 21. SEM image of Cu-4G worn surface.

However, adhesive wear characteristics are not observed on the wear surface. This can be probably related to not smearing graphite particles over the surface in early stages of sliding so that adhesive wear has occurred at first and before delamination and accordingly a small amount of copper has transferred to wear disk. Although, continuing sliding and so smearing graphite particles over the surface and also squeezing particles out from subsurface area to the wear surface stop adhesive wear.

Consequently, increase in graphite content results in increase in delamination wear and decrease in adhesive wear. Also, increase in graphite content lead to increase in pores quantities and so decrease in their distances. Therefore, these pores and resultant cracks join together faster and thus; the size of the debris is decreased.

4. Conclusions

1. Fabrication of copper–graphite composites by friction stir processing (FSP) is possible. Using this technique leads to more homogenous distribution of particles in surface of composite and prevents particle changing into clusters which was the most important problem in prior techniques such as powder metallurgy and centrifugal casting. It should be noted that in order to produce more heat and avoid wasting produced heat, rotating speed and transverse speed should be chosen high and low respectively and specimens should be isolated.
2. Using tool with triangular pin leads to better distribution of particle rather than other tools which are because of flow pattern of materials against this tool. The area of composite produced with this tool is larger in comparison with composites produced by other tools.
3. Friction coefficient is dramatically decreased with increase in graphite content so that friction coefficient of Cu-4G composite containing about 22 vol% graphite is 79% lower than pure

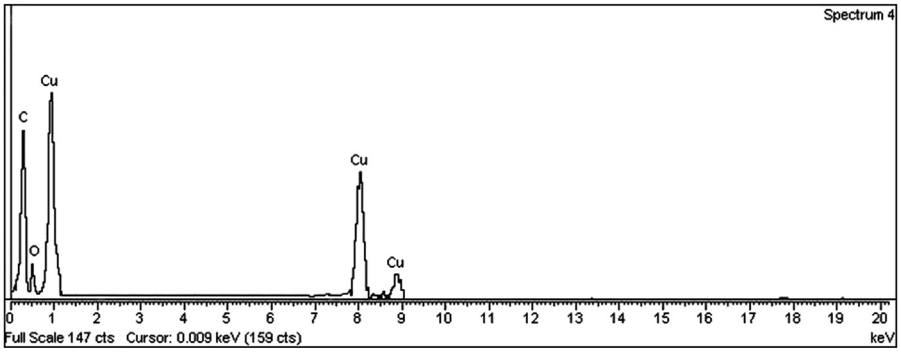

Fig. 22. EDS analysis of Cu-4G worn surface.

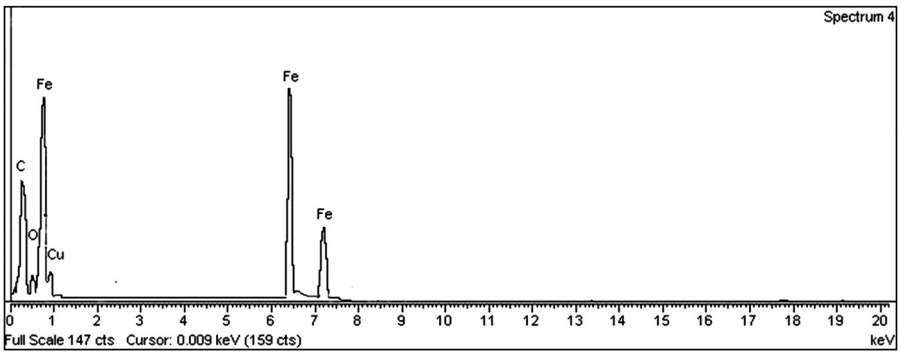

Fig. 23. EDS analysis of counterpart (wear disk) running against Cu-4G pin.

annealed copper. This is due to presence of graphite as a solid lubricant and decrease in number of metal to metal contact point.

4. Friction coefficient decreases to some extent as graphite content increases and after a threshold value of graphite content, it remains constant. The threshold graphite content in this study is about 25 vol%.
5. Wear loss of specimens is decreased with increase in graphite content. Adding about 22 vol% graphite to copper increases wear resistance of the composite by 65%. This is due to presence of graphite as a solid lubricant.
6. Increase in graphite content results in increase in delamination wear and decrease in adhesive wear.

References

[1] W.M. Thomas, E.D. Nicholas, J.C. Needham, M.G. Murch, P. Temple smith, C.J. Dawes, G.B. Patent Application No. 9125978.8, 1991.

[2] R.S. Mishra, Z.Y. Ma, Friction stir welding and processing, Materials Science and Engineering: R: Reports 50 (2005) 1–78.

[3] R.S. Mishra, M.W. Mahoney, S.X. McFadden, N.A. Mara, A.K. Mukherjee, High strain rate superplasticity in a friction stir processed 7075 Al alloy, Scripta Materialia 42 (2000) 163–168.

[4] R.S. Mishra, M.W. Mahoney, Friction stir processing: a new grain refinement technique to achieve high strain rate superplasticity in commercial alloys, Materials Science Forum 357–359 (2001) 507–514 12.

[5] R.S. Mishra, Z.Y. Ma, I. Charit, Friction stir processing: a novel technique for fabrication of surface composite, Materials Science and Engineering: A 341 (2003) 307–310.

[6] Y. Morisada, H. Fujii, T. Nagaoka, M. Fukusumi, MWCNTs/AZ31 surface composites fabricated by friction stir processing, Materials Science and Engineering: A 419 (2006) 344–348.

[7] A. Shafiei-Zarghani, S.F. Kashani-Bozorg, A. Zarei-Hanzaki, Microstructures and mechanical properties of Al/Al_2O_3 surface nano-composite layer produced by friction stir processing, Materials Science and Engineering: A 500 (2009) 84–91.

[8] W. Wang, Q.Y. Shi, P. Liu, H.K. Li, T. Li, A novel way to produce bulk SiCp reinforced aluminum metal matrix composites by friction stir processing, Journal of Materials Processing Technology 209 (2009) 2099–2103.

[9] C.J. Lee, J.C. Huang, P.J. Hsieh, Mg based nano-composites fabricated by friction stir processing, Scripta Materialia 54 (2006) 1415–1420.

[10] M. Kestursatya, J.K. Kim, P.K. Rohatgi, Wear performance of copper–graphite composite and a leaded copper alloy, Materials Science and Engineering: A 339 (2003) 150–158.

[11] S.F. Moustafa, S.A. El-Badry, A.M. Sanad, B. Kieback, Friction and wear of copper–graphite composites made with Cu-coated and uncoated graphite powders, Wear 253 (2002) 699–710.

[12] H. Kato, M. Takama, Y. Iwai, K. Washida, Y. Sasaki, Wear and mechanical properties of sintered copper–tin composites containing graphite or molybdenum disulfide, Wear 255 (2003) 573–578.

[13] P.K. Rohatgi, S. Ray, Y. Liu, Tribological properties of metal matrix graphite particle composites, International Metallurgical Reviews 37 (1992) 129–149.

[14] J. Kovacik, S. Emmer, J. Bielek, L. Kelesi, Effect of composition on friction coefficient of Cu–graphite composites, Wear 265 (2008) 417–421.

[15] K. Rajkumar, S. Aravindan, Tribological behavior of microwave processed copper–nanographite composites, Tribology International 57 (2013) 282–296.

[16] X. Jincheng, Y. Hui, X. long, L. Xiaolong, Y. Hua, Effects of some factors on the tribological properties of the short carbon fiber-reinforced copper composite, Materials & Design 25 (2004) 489–493.

[17] Y. Tang, H. Liu, H. Zhao, L. Liu, Y. Wu, Friction and wear properties of copper matrix composites reinforced with short carbon fibers, Materials & Design 29 (2008) 257–261.

[18] J. Jinlong, D. Jianfeng, Y. Hua, W. Qing, Effects of some factors on the tribological properties of the short carbon fiber-reinforced copper composite, Materials & Design 25 (2004) 489–493.

[19] Z. Jun, X. Jincheng, H. Wei, X. Long, D. Xiaoyan, W. Sen, T. Peng, M. Xiaoming, Y. Jing, J. Chao, L. Lei, Wear performance of the lead free tin bronze matrix composite reinforced by short carbon fibers, Applied Surface Science 255 (2009) 6647–6651.

[20] L. Xia, B. Jia, J. Zeng, J. Xu, Wear and mechanical properties of carbon fiber reinforced copper alloy composites, Materials Characterization 60 (2009) 363–369.

[21] Y. Zhan, G. Zhang, The role of graphite particles in the high-temperature wear of copper hybrid composites against steel, Materials & Design 27 (2006) 79–84.

[22] J.K. Kim, M. Kestursatya, P.K. Rohatgi, Tribological properties of centrifugally cast copper alloy–graphite particle composite, Metallurgical and Materials Transactions A 31A (2000) 1283–1293.

[23] B. Zahmatkesh, M.H. Enayati, A novel approach for development of surface nanocomposite by friction stir processing, Materials Science and Engineering: A 527 (2010) 6734–6740.

[24] K. Elangovan, V. Balasubramanian, Influences of pin profile and rotational speed of the tool on the formation of friction stir processing zone in AA2219 aluminum alloy, Materials Science and Engineering: A 459 (2007) 7–18.

[25] Z.Y. Ma, Friction stir processing technology: a review, Metallurgical and Materials Transactions A 39 (2008) 1–17.

[26] Y.S. Zhang, Z. Han, K. Wang, K. Lu, Friction and wear behaviors of nanocrystalline surface layer of pure copper, Wear 260 (2006) 942–948.